Parameter Design of Conformal PML Based on 2D Monostatic RCS Optimization

Y. J. Zhang* and X. F. Deng

Northwestern Polytechnical University, Xi'an, 710072, P.R. China
*zyj19191@nwpu.edu.cn

Abstract – In this study, 2D finite element (FE) solving process with the conformal perfectly matched layer (PML) is elucidated to perform the electromagnetic scattering computation. With the 2D monostatic RCS as the optimization objective, a sensitivity analysis of the basic design parameters of conformal PML (e.g., layer thickness, loss factor, extension order and layer number) is conducted to identify the major parameters of conformal PML that exerts more significant influence on 2D RCS. Lastly, the major design parameters of conformal PML are optimized by the simulated annealing algorithm (SA). As revealed from the numerical examples, the parameter design and optimization method of conformal PML based on SA is capable of enhancing the absorption effect exerted by the conformal PML and decreasing the error of the RCS calculation. It is anticipated that the parameter design method of conformal PML based on RCS optimization can be applied to the cognate absorbing boundary and 3D electromagnetic computation.

Index Terms – 2D conformal PML, monostatic RCS, parameters optimization, sensitivity analysis, simulated annealing algorithm.

I. INTRODUCTION

In FE computation for the electromagnetic scattering, the local boundary condition refers to the most extensively employed open-domain boundary condition. As the scattering target turns larger and more sophisticated, the more rigorous requirement of local boundary condition are raised. How to build a high-performance local boundary condition, save the spatial scattering elements and enhance the solution efficiency of finite element method (FEM) has always been the hotspot in open-domain electromagnetic scattering computation study. Perfectly matched layer (PML) [1-3] refers to the optimal local boundary condition over the past few years. Theoretically, the absorption effect of PML is only determined by the thickness and the number of layers of PML for the electromagnetic wave that exhibits an arbitrary frequency and an incident angle. Moreover, the conformal PML (CPML) does not disturb the sparsity of the system matrix, i.e., a property to effectively store and solve the FEM solution of electromagnetic scattering. Though the rectangular (2D) or block (3D) PML [4-10] turns into the popular mesh truncation boundary, a more efficient conformal PML [11-13] absorbing boundary is built for the larger size and more complex scattering targets. The conformal method is capable of generating the mesh truncation boundary that is consistent with the shape of scatterers to minimize the scattering space between scatterers and absorbing boundaries; thus, conformal PML can effectively save the spatial scattering elements and enhance the solution efficiency of FEM [14-17]. Accordingly, why conformal PML constantly arouses the attention from researchers is explained. Due to the above advantages and its outstanding role in the finite element scattering computation, the conformal PML is selected as the optimization design object, and the absorption effect and calculation efficiency of conformal PML are expected to be improved through the parametric design and RCS optimization algorithm proposed in this paper. Moreover, it is hoped that this study can provide some research ideas and exploration direction for the optimization design of cognate absorbing boundary conditions.

In this study, to enhance the absorbing efficiency of conformal PML and reduce the error of RCS calculation, a method is proposed in the present study to optimize the basic parameters of 2D conformal PML by the simulated annealing algorithm. By typical numerical cases, the availability and feasibility of the optimization design method are verified. Considering its good availability and applicability, the optimization design method in this paper can be extended from 2D electromagnetic computation to 3D electromagnetic computation.

II. FE SOLUTION OF 2D ELECTROMAGNETIC SCATTERING WITH CONFORMAL PML

Overall, the open domain electromagnetic scattering problem can be addressed in the region surrounded by the conformal PML. The conformal PML can be considered a shell composed of lossy anisotropic media,

Submitted On: February 18, 2021
Accepted On: July 7, 2021

https://doi.org/10.47037/2020.ACES.J.360614

exhibiting geometric similarity to the outer surface of scatterers. In the construction of conformal PML (Fig. 1), the surface near the scatterer is termed as the inner surface; besides, the outermost surface away from scatterers is called the outer surface or back surface. On the whole, the conformal PML is designed as the multi-layer shells exhibiting different thicknesses to exhibit a high absorbing efficiency. In the region of conformal PML, the permeability and permittivity are respectively expressed as $\overline{\overline{\mu}}=\mu_r\overline{\overline{\Lambda}}$ and $\overline{\overline{\varepsilon}}=\varepsilon_r\overline{\overline{\Lambda}}$. In the local coordinate system (ξ_1,ξ_2,ξ_3), the constitutive parameters of conformal PML are defined in the complex stretching [14, 18]:

$$\overline{\overline{\Lambda}}_{\xi_1,\xi_2,\xi_3}=\begin{bmatrix}\frac{s_2s_3}{s_1} & 0 & 0\\ 0 & \frac{s_1s_3}{s_2} & 0\\ 0 & 0 & \frac{s_1s_2}{s_3}\end{bmatrix}_{\xi_1,\xi_2,\xi_3}, \tag{1}$$

$$\begin{cases} s_1=\left(r_{01}+\tilde{\xi}\right)/r_1\\ s_2=\left(r_{02}+\tilde{\xi}\right)/r_2\\ s_3=s=1-j\delta\left(\frac{\xi_3}{t}\right)^m,\\ \tilde{\xi}=\int_0^{\xi_3}s(\zeta)\mathrm{d}\zeta \end{cases} \tag{2}$$

where ξ_1,ξ_2,ξ_3 denote orthogonal local coordinate components; r_{01} and r_{02} represent the principal radiuses of curvature of a given point on the inner surface of conformal PML [14]; $r_1=r_{01}+\xi_3$ and $r_2=r_{02}+\xi_3$ refer to the principal radiuses of curvature of point lengthened ξ_3 following the outer normal direction of the given point; *s* indicates the complex stretching variable [14] in the ξ_3 direction; *t* is the total thickness of the conformal PML; δ is the loss factor of the conformal PML; *m* represents the extension order of complex extension variable in the conformal PML.

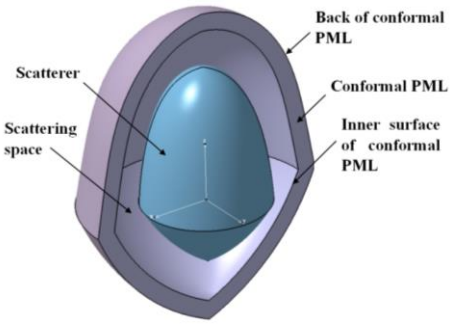

Fig. 1. The construction of a conformal PML.

In the 2D case, assuming that the local coordinate axis direction ξ_3 complies with the *z*-axis direction of the global coordinate system; the parameters of the conformal PML remains constant along the z-axis direction; the constitutive parameters [15] of conformal PML are defined as:

$$\overline{\overline{\Lambda}}_{x,y,z}=\begin{bmatrix}\tilde{\Lambda} & 0\\ 0 & \beta\end{bmatrix}, \tag{3}$$

$$\tilde{\Lambda}=\tilde{J}^t\begin{bmatrix}\alpha & 0\\ 0 & 1/\alpha\end{bmatrix}\tilde{J}, \tag{4}$$

where $\tilde{\Lambda}$ denotes a 2 × 2 submatrix; $\tilde{J}$ represents the Jacobi matrix of 2D coordinate transformation. $\alpha=s_2/s_1$ and $\beta=s_1s_2$.

The following derivation is expressed based on the electric field E_z. By substituting (4) into the wave equation of 2D electromagnetic scattering problem, the wave equation [15] with the conformal PML is expressed:

$$\nabla\bullet\left[\frac{1}{\mu_r}\tilde{\Lambda}\nabla E_z\right]+k_0^2\beta E_z{}^2=0. \tag{5}$$

The corresponding functional expression is written as:

$$F\left(\boldsymbol{E}^s\right)=\frac{1}{2}\iint_\Omega\left(\frac{1}{\mu_r}\nabla E_z\bullet\tilde{\Lambda}\bullet\nabla E_z-k_0^2\beta E_z{}^2\right)d\Omega. \tag{6}$$

Thus, in the conformal PML region Ω, the element matrix is expressed as:

$$K_{lk}^e=\iint_\Omega\left[\frac{1}{\mu_r}\nabla N_l^e\bullet\tilde{\Lambda}\bullet N_k^e-k^2\beta N_l^e\bullet N_k^e\right]d\Omega. \tag{7}$$

If the triangular element is employed for the region discretization, the matrix elements in (7) are expressed as follows:

$$\begin{cases} K_{11}^e=\frac{l_{12}^el_{12}^e}{\Delta^e}\left[\frac{1}{\mu_r^e}\alpha^e-\frac{k_0^2\varepsilon_r^e\beta^e}{24}\left(f_{11}^e+f_{22}^e-f_{12}^e\right)\right]\\ K_{22}^e=\frac{l_{23}^el_{23}^e}{\Delta^e}\left[\frac{1}{\mu_r^e}\alpha^e-\frac{k_0^2\varepsilon_r^e\beta^e}{24}\left(f_{22}^e+f_{33}^e-f_{23}^e\right)\right]\\ K_{33}^e=\frac{l_{13}^el_{13}^e}{\Delta^e}\left[\frac{1}{\mu_r^e}\alpha^e-\frac{k_0^2\varepsilon_r^e\beta^e}{24}\left(f_{11}^e+f_{33}^e-f_{13}^e\right)\right]\\ K_{12}^e=\frac{l_{12}^el_{23}^e}{\Delta^e}\left[\frac{1}{\mu_r^e}\alpha^e-\frac{k_0^2\varepsilon_r^e\beta^e}{48}\left(f_{12}^e+f_{23}^e-2f_{13}^e-f_{22}^e\right)\right]\\ K_{13}^e=\frac{l_{12}^el_{13}^e}{\Delta^e}\left[\frac{1}{\mu_r^e}\alpha^e-\frac{k_0^2\varepsilon_r^e\beta^e}{48}\left(f_{12}^e+f_{13}^e-2f_{23}^e-f_{11}^e\right)\right]\\ K_{23}^e=\frac{l_{13}^el_{23}^e}{\Delta^e}\left[\frac{1}{\mu_r^e}\alpha^e-\frac{k_0^2\varepsilon_r^e\beta^e}{48}\left(f_{13}^e+f_{23}^e-2f_{12}^e-f_{33}^e\right)\right] \end{cases}, \tag{8}$$

where Δ^e denotes the area of element; l_{ij}^e represents the constant coefficient of element; f_{ij}^e is the source function of element. For the specific calculation formula, please refer to [19].

From the theoretical perspective, the electromagnetic wave is completely absorbed at the back surface of the conformal PML, which is expressed as:

$$E_z\big|_{\Gamma_{CPML}} = 0, \tag{9}$$

where Γ_{CPML} denotes the boundary of back surface of the conformal PML. If the scatterer acts as a conductor, the incident electromagnetic wave is overall reflected. Thus, Dirichlet boundary conditions should be set on the scatterer surface.

After the mentioned element matrixes are assembled to form the global matrix [k] and the corresponding boundary conditions and incident conditions are substituted, the system equations as written in (10) can be solved to yield the electric field distribution:

$$[K]\{E_z\} = \{b\}. \tag{10}$$

The electric field solved is adopted to calculate the single station RCS:

$$\sigma = \lim_{\rho\to\infty} 2\pi\rho \frac{\left|E^{sc}\right|^2}{\left|E^{inc}\right|^2} = \lim_{\rho\to\infty} 2\pi\rho \frac{\left|H^{sc}\right|^2}{\left|H^{inc}\right|^2}. \tag{11}$$

The normalized RCS can be a popular expression:

$$\sigma/\lambda = 10\lg(\sigma/\lambda). \tag{12}$$

III. NUMERICAL CASE

In the present study, the incident plane electromagnetic waves are defined as:

$$\Phi^{inc} = e^{jk_0\left(x\cos\varphi^{inc} + y\sin\varphi^{inc}\right)}, \tag{13}$$

where φ^{inc} denotes the incident angle. The wavelength of incident plane electromagnetic waves is expressed as λ.

To subsequently optimize the parameter of 2D conformal PML, three numerical cases are presented in this section based on two typical 2D scatterers.

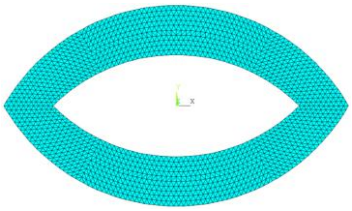

Fig. 2. Meshed ovate.

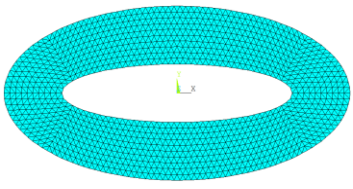

Fig. 3. Meshed ellipse.

Case 1: As shown in Fig. 2, the width and thickness of conducting ovate are 5 λ and 2.07 λ, respectively. The scattering area (the distance between the inner surface of conformal PML and the surface of scatterer) exhibits the thickness of 0.5 λ. The mesh size reaches 0.05 λ.

Case 2: Like the Fig. 2, the width and thickness of conducting ovate are 15 λ and 2.14 λ respectively. The thickness of scattering area is 0.5 λ. The mesh size is 0.05 λ.

Case 3: As shown in Fig. 3, the major and minor axes of conducting ellipse are λ and 0.5 λ, respectively. The scattering area exhibits the thickness of 0.5 λ. The mesh size is 0.05 λ.

IV. SENSITIVITY ANALYSIS OF 2D RCS

As indicated from the deduction in the Section II, the basic designed parameters of conformal PML affecting RCS are the loss factor δ, extension order *m*, layer thickness *d* and layer number *n*, i.e.,

$$\sigma \sim f(\delta, m, d, n). \tag{14}$$

To explore the effect of these basic parameters on 2D RCS, a sensitivity analysis for three numerical cases in the Section III is conducted with the central difference method. The basic formula is expressed as:

$$\begin{aligned} F'(x_i) &= \frac{F(x_i+h) - F(x_i-h)}{2h} + O(h^2) \\ &\approx \frac{F(x_i+h) - F(x_i-h)}{2h}, \end{aligned} \tag{15}$$

where the step size *h* is set to 1% of the corresponding parameter. The sensitivity function $F(x_i)$ can be considered the RCS σ in (14), while the variables x_i can be considered one of the loss factor δ, extension order *m*, layer thickness *d* and layer number *n* in (14).

Supposed that the wavelength of incident electromagnetic wave is set to λ=0.01*m* (only to provide an exact input for program operation), the initial basic parameters of conformal PML are set as δ=10, *m*=2, $d_i = 0.05\lambda$, *n*=6, and the disturbance step size is set to *h*=1% for the initial basic parameters of conformal PML, the sensitivity function $F(x_i)$ can be calculated as listed in Tables 1, 2, 3 at the different incident angles φ^{inc}. For example, in the sensitivity analysis process of case 1, the disturbance 1% of loss factor at incident angle 0^0 is substituted into (15), thus the sensitivity response of RCS at incident angle 0^0 will be obtained shown as the second row, second column cell of Table 1. In the same way, the sensitivity responses of RCS at the other incident angle will be calculated and listed in the second column of Table 1 for the disturbance 1% of loss factor. Similarly, the sensitivity responses of RCS for the disturbance 1% of extension order, layer thickness and layer number respectively can be obtained shown as the third, fourth and fifth column of Table 1. Repeat the

above sensitivity analysis process and the results are shown in tables 2 and 3.

Obviously, for the 2D RCS with the conformal PML, the most influential parameter is layer thickness, while the effects of other parameters are relatively small. Accordingly, the thickness of each layer will be adopted as the main design variables for the RCS optimization. Since the loss factor and extension order are the vital design parameters of conformal PML, the loss factor and extension order are still selected as design variables to exhibit the optimal absorbing efficiency in the optimization analysis of next section. Theoretically, the more conformal PML layers (more absorbing media) will bring the better absorbing effect. However, with the increase of the layer number of conformal PML, the interlayer reflection error and the element number of conformal PML also raise. Trading off the absorbing effect, interlayer reflection error and the element number of conformal PML, here the layer number of conformal PML is set to 6.

Table 1: Sensitivity analysis results of case 1

Incident Angle/(°)	Loss Factor	Extension Order	Layer Thickness	Layer Number
0	-0.0216	0.1085	-4.1254	0.0391
5	0.0513	-0.1012	-1.7991	-0.0391
10	0.0806	-0.2090	30.6554	-0.0797
15	0.0065	-0.0235	-30.6450	-0.0083
20	-0.0338	0.0897	-70.2444	0.0353
25	0.0533	-0.0205	11.7344	-0.0138
30	-0.0167	0.0413	39.6296	0.0162
35	-0.0352	0.0790	0.1706	0.0295
40	0.0065	-0.0193	-14.6755	-0.0068
45	-0.0076	0.0314	6.4041	0.0115
50	0.0002	0.0012	36.7430	0.0002
55	0.0095	-0.0301	32.3789	-0.0110
60	-0.0025	0.0065	-8.8950	0.0027
65	-0.0110	0.0319	-27.2776	0.0118
70	-0.0059	0.0204	64.2721	0.0072
75	0.0003	-0.0007	-24.4353	-0.0005
80	0.0100	-0.0304	-22.0506	-0.0115
85	0.0097	-0.0307	-34.9960	-0.0115
90	0.0133	-0.0409	20.5271	-0.0152

Table 2: Sensitivity analysis results of case 2

Incident Angle/(°)	Loss Factor	Extension Order	Layer Thickness	Layer Number
0	0.0138	-0.0023	-9.2754	0.0078
5	-0.0007	0.0001	-50.3808	0.0029
10	-0.0010	0.0002	-89.3209	-0.0032
15	-0.0022	0.0004	85.3498	-0.0150
20	-0.0008	0.0001	-132.4588	0.0681
25	0.0020	-0.0003	41.3835	-0.0079
30	-0.0031	0.0005	11.0661	0.0107
35	-0.0019	0.0003	-12.1974	-0.0131
40	-0.0012	0.00018	-39.7161	0.0214
45	-0.0010	0.0002	20.7344	-0.0048
50	-0.0007	0.0001	-7.0409	-0.0044
55	0.0002	-0.00001	-13.4454	-0.0018
60	0.0002	-0.00001	5.4368	0.00005
65	-0.0003	0.00001	-12.5664	0.0004
70	0.0003	-0.000002	-10.9907	0.0006
75	-0.0002	0.00001	1.6422	0.0006
80	0.0001	0.0002	5.3411	-0.0015
85	-0.00001	0.00001	-9.9341	0.0004
90	0.0001	-0.00001	16.2334	-0.0007

Table 3: Sensitivity analysis results of case 3

Incident Angle/(°)	Loss Factor	Extension Order	Layer Thickness	Layer Number
0	0.0480	-0.2231	4.5503	-0.0810
5	0.0479	-0.2239	-17.1200	-0.0808
10	0.0467	-0.2201	52.8826	-0.0784
15	0.0393	-0.1881	27.5349	-0.0654
20	0.0243	-0.1191	0.7037	-0.0396
25	0.0064	-0.0358	-46.5160	-0.0097
30	-0.0086	0.0357	20.2953	0.0149
35	-0.0176	0.0816	-27.5811	0.0297
40	-0.0176	0.0877	-96.7805	0.0303
45	-0.0106	0.0588	52.7488	0.0192
50	-0.0029	0.0189	2.0418	0.0050
55	0.0053	-0.0305	2.5652	-0.0116
60	0.0111	-0.0653	-32.7123	-0.0225
65	0.0082	-0.0476	-16.9139	-0.0153
70	-0.0001	0.0003	-4.4872	0.0013
75	-0.0069	0.0386	-11.6805	0.0140
80	-0.0096	0.0535	-21.9851	0.0185
85	0.0098	0.0551	-75.5233	0.0186
90	-0.0100	0.0558	19.6414	0.0187

V. OPTIMIZATION ANALYSIS OF 2D RCS

Given the sensitivity analysis results in the previous section, the thickness of each layer d_i, loss factor δ and extension order m are employed as the optimization design variables. The optimization process aims to minimize the average error of 2D RCS calculated by the conformal PML and ABC absorbing boundary (the solution results with the conventional ABC absorbing boundary are considered the baseline). For the geometric symmetry of the examples, the incident angle is set to $0^\circ \sim 90^\circ$. To enhance the calculation accuracy, the incident angle interval is set to 1°. Accordingly, the optimization function is expressed as:

$$f\left(d_i,\delta,m\right)=\frac{\sum_{i=0^\circ}^{i=90^\circ}\left|\sigma_{\mathrm{CPML}}-\sigma_{\mathrm{ABC}}\right|}{91}. \tag{16}$$

The constraints are set as follows:

$$\begin{cases}0.05\lambda \le d_i \le 0.5\lambda \\ 1\le \delta \le 100 \\ 1\le m\le 20\end{cases}. \tag{17}$$

Given the efficiency and the stability of the optimization iteration, the simulated annealing algorithm (SA) [20] exhibiting the high stability in the global optimization algorithms is employed to search the optimal parameters of conformal PML. The optimization flow chart is illustrated in Fig. 4.

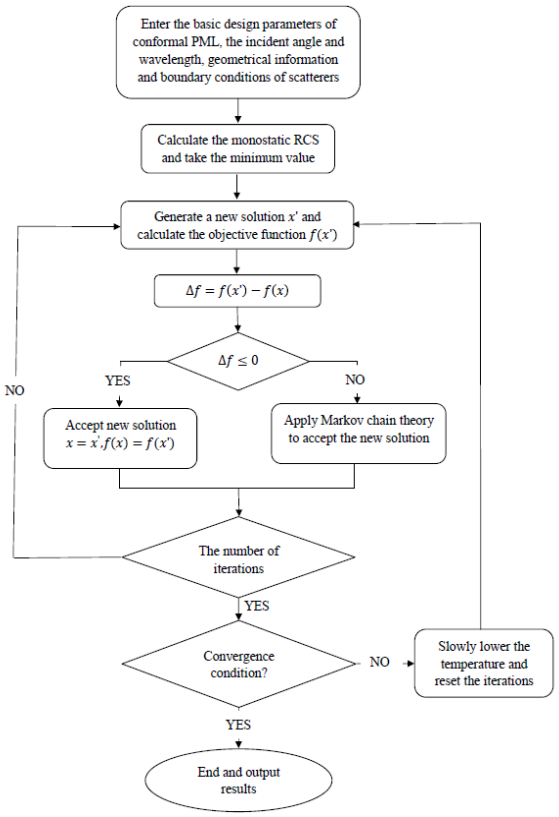

Fig. 4. SA optimization flowchart of 2D RCS with the conformal PML.

As indicated in the flow chart, the optimization program is compiled and run in MATLAB. Considering that the computation time cost for optimization will vary with the computer hardware configuration, here the number of iterations is used to show the optimization process and calculation efficiency. The optimization processes of three numerical cases are illustrated in Figs. 5, 6, 7. It is obvious that for the different shape and size scatterers (case 1, 2, 3), SA optimization algorithm can enter the convergence state in 100 iterations and obtain the convergence solution in 200 iterations. Moreover, the convergence process of SA optimization algorithm is very smooth. Therefore, SA algorithm can be applied into the RCS optimization solution of complex and 3D scatterers.

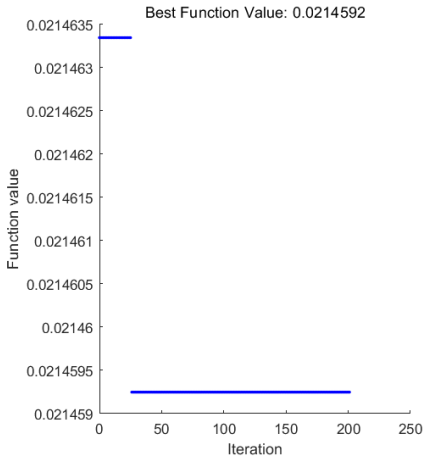

Fig. 5. RCS optimization process of case 1.

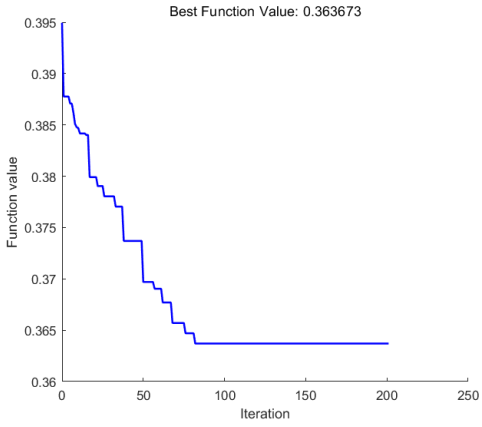

Fig. 6. RCS optimization process of case 2.

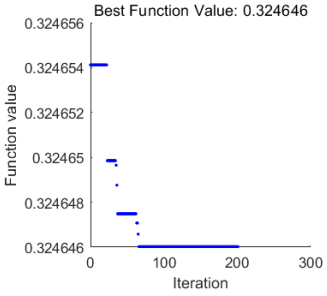

Fig. 7. RCS optimization process of case 3.

In Figs. 8, 9, 10, the 2D Monostatic RCS before and after the optimization for three numerical cases are compared with the conventional ABC absorbing boundary [19]. The parameter optimization results of 2D conformal PML are listed in Table 4. Table 5 lists the average errors of 2D monostatic RCS calculated by the conformal PML and ABC absorbing boundary. As revealed from the results, for the different shape and size scatterers (case 1, 2, 3), 2D monostatic RCS with the conformal PML after optimization is closer to the RCS with the ABC absorbing boundary compared with the RCS with the conformal PML before optimization. The main reason is that SA algorithm can search the optimal parameters of conformal PML to minimize the interlayer reflection error and the average error of RCS calculated with the conformal PML and ABC absorbing boundary at the different incident angles. Therefore, the parameters optimization method of conformal PML based on SA is capable of obviously reducing the error, and the RCS calculation results with the optimized conformal PML are more consistent with the calculation results that exhibit the ABC absorbing boundary.

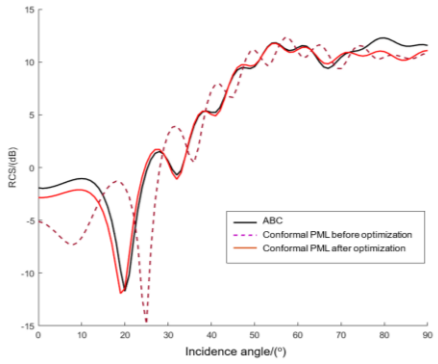

Fig. 8. 2D monostatic RCS before and after the optimization for case 1.

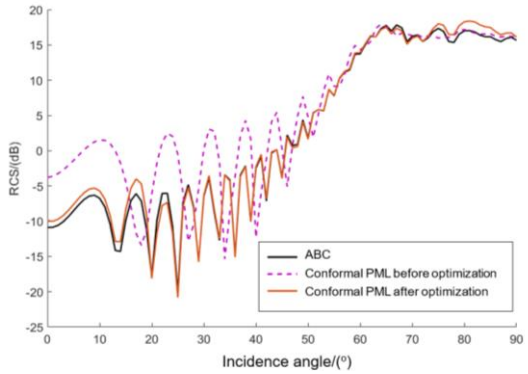

Fig. 9. 2D monostatic RCS before and after the optimization for case 2.

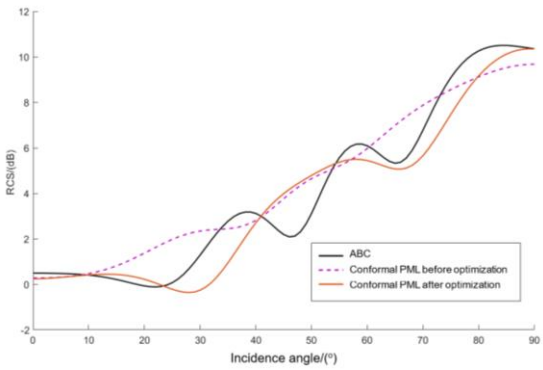

Fig. 10. 2D monostatic RCS before and after the optimization for case 3.

Table 4: Parameter optimization results of 2D conformal PML

Opti.	Layer Thickness/(*λ)						Loss Factor	Extension Order
	1st Layer	2nd Layer	3rd Layer	4th Layer	5th Layer	6th Layer		
Initial	0.05	0.05	0.05	0.05	0.05	0.05	13	2
Example 1	0.0727	0.4746	0.4538	0.4769	0.4582	0.3865	5.9995	3.8061
Example 2	0.1248	0.4868	0.0711	0.0500	0.0841	0.1219	94.2601	1.5402
Example 3	0.0508	0.3656	0.3655	0.4369	0.3536	0.1923	26.9301	15.8849

Table 5: Average errors of 2D monostatic RCS calculated by the conformal PML and ABC

Errors	Example 1		Example 2		Example 3	
	Before Opti.	After Opti.	Before Opti.	After Opti.	Before Opti.	After Opti.
Average error/(dB)	2.5399	0.0214	2.8547	0.3637	1.2343	0.3246
Reduction percentage of average error /(%)	99.1574		87.2596		73.7017	

VI. CONCLUSION

In the present study, the constitutive parameters of 2D conformal PML and FE solving process of electromagnetic scattering with the conformal PML are elucidated. For three numerical cases based on two 2D scatterers whose shapes are originating from the typical scattering targets [19], the sensitivity analysis of the basic design parameters of conformal PML (e.g., layer thickness, loss factor, extension order and layer number) is conducted by applying the 2D monostatic RCS as the objective function. Given the results of sensitivity analysis, the thicknesses of each layer are taken as the major optimization design parameters. Since the loss factor and extension order are also the vital design parameters of conformal PML, the loss factor and extension order are still considered the design variables in the optimization analysis. Lastly, the optimized design parameters of conformal PML with small calculation errors and high absorbing efficiency are conducted with the optimization method based on SA algorithm. Sequentially, the 2D monostatic RCS before and after the optimization for three numerical cases are compared with the conventional ABC absorbing boundary. The numerical results suggest that the parameter optimization method of conformal PML proposed in the present study possesses the high absorbing performance, also can provide the optimization scheme and technical reference for parameter design of cognate absorbing boundary and 3D electromagnetic computation.

ACKNOWLEDGEMENT

This work was supported by National Science Foundation for Distinguished Young Scholars of China (11201375), Specialized Research Fund for the Doctoral Program of Higher Education of China (20106102120001) and Postdoctoral Science Foundation of China (201003680).

REFERENCES

[1] J. P. Berenger, "A perfectly matched layer for the absorption of electromagnetic waves," *Journal of Computational Physics*, vol. 114, no. 2, pp. 185-200, 1994.

[2] C. Wu, E. A. Navarro, P. Y. Chung, and J. Litva, "Modeling of waveguide structures using the nonorthogonal FDTD method with a PML absorbing boundary," *Microwave and Optical Technology Letters*, vol. 8, no. 4, pp. 226-228, 1995.

[3] W. C. Chew and J. M. Jin, "Perfectly matched layer in the discretized space: an analysis and optimization," *Electromagnetics*, vol. 16, no. 4, pp. 325-340, 1996.

[4] S. D. Gedney, "An anisotropic perfectly matched layer-absorbing medium for the truncation of FDTD lattices," *IEEE Transactions on Antennas and Propagation*, vol. 44, no. 12, pp. 1630-1639, 1996.

[5] J. P. Berenger, *Perfectly Matched Layer (PML) for Computational Electromagnetics*, Morgan & Claypool, 2014.

[6] Z. Lou, D. Correia, and J.-M. Jin, "Second-order perfectly matched layers for the time-domain finite-element method," *IEEE Transactions on Antennas and Propagation*, vol. 55, no. 3, pp. 1000-1004, 2007.

[7] Z. S. Sacks, D. M. Kingsland, R. Lee, and J. F. Lee, "A perfectly matched anisotropic absorber for use as an absorbing boundary condition," *IEEE Transactions on Antennas and Propagation*, vol. 43, no. 12, pp. 1460-1463, 1995.

[8] O. Ozgun and M. Kuzuoglu, "Iterative leap-field domain decomposition method: A domain decomposition finite element algorithm for 3D electromagnetic boundary value problems," *IET Microwaves Antennas & Propagation*, vol. 4, no. 4, pp. 543-552, 2010.

[9] Y. Xiao and Y. Lu, "Combination of PML and ABC for scattering problem," *IEEE Transactions on Magnetics*, vol. 37, no. 5, pp. 3510-3513, 2001.

[10] M. Movahhedi, A. Abdipour, H. Ceric, A. Sheikholeslami, and S. Selberherr, "Optimization of the perfectly matched layer for the finite-element time-domain method," *IEEE Microwave and Wireless Components Letters*, vol. 17, no. 1, pp. 10-12, 2007.

[11] O. Ozgun and M. Kuzuoglu, "Recent advances in perfectly matched layers in finite element applications," *Turkish Journal of Electrical Engineering and Computer Sciences*, vol. 16, no. 1, pp. 57-66, 2008.

[12] B. Donderici and F. L. Teixeira, "Conformal perfectly matched layer for the mixed finite element time-domain method," *IEEE Transactions on Antennas and Propagation*, vol. 56, no. 4, pp. 1017-1026, 2008.

[13] M. Kuzuoglu, B. B. Dundar, and R. Miitra, "Conformal perfectly matched absorbers in finite element mesh truncation," *IEEE Antennas and Propagation Society International Symposium Digest*, vol. 2, pp. 1176-1179, 2000.

[14] P. Liu, J. D. Xu, and W. Wan, "A finite-element realization of a 3D conformal PML," *Microwave and Optical Technology Letters*, vol. 30, no. 3, pp. 170-173, 2001.

[15] P. Liu, "Investigation of PML for the Finite Element Analysis of Electromagnetic Scattering Problem," *Doctoral Thesis, Northwest Polytechnic University*, 2001.

[16] T. Rylander and J. M. Jin, "Conformal perfectly matched layers for the time domain finite element method," *IEEE Antennas and Propagation Society International Symposium Digest*, vol. 1, pp. 698-701, 2003.

[17] F. L. Teixeira, K. P. Hwang, W. C. Chew, and J.-M. Jin, "Conformal PML-FDTD schemes for electromagnetic field simulations: A dynamic stability study," *IEEE Transactions on Antennas and Propagation*, vol. 49, no. 6, pp. 902-907, 2001.

[18] Y. J. Zhang and X. H. Zhang, "Normal directional NURBS arithmetic of conformal PML," *Applied Computational Electromagnetics Society Journal*, vol. 29, no. 11, pp. 904-910, 2014.

[19] J. M. Jin. *The Finite Element Method in Electromagnetics*, Third Edition. Hoboken, NJ: Wiley, 2014.

[20] J. Awange, B. Paláncz, R. Lewis, and L. Völgyesi, *Mathematical Geosciences: Hybrid Symbolic-Numeric Methods*, AG: Springer, 2018.